

# UPCommons

## Portal del coneixement obert de la UPC

<http://upcommons.upc.edu/e-prints>

This is the accepted version of the following article: Waseem, W. [et al.]. Restricted Hilbert Transform for Non-Hermitian Management of Fields. "Physical Review Applied", 7 Octubre 2020, vol. 14, núm. 4, 044010. DOI: <[10.1103/PhysRevApplied.14.044010](https://doi.org/10.1103/PhysRevApplied.14.044010)>

# Restricted Hilbert transform for non-Hermitian management of fields

W. W. Ahmed<sup>1</sup>, R. Herrero<sup>2</sup>, M. Botey<sup>2</sup>, Y. Wu<sup>1\*</sup>, and K. Staliunas<sup>2,3†</sup>

<sup>1</sup>*Division of Computer, Electrical and Mathematical Sciences and Engineering, King Abdullah University of Science and Technology (KAUST), Thuwal, 23955-6900, Saudi Arabia*

<sup>2</sup>*Departament de Física, Universitat Politècnica de Catalunya (UPC), Colom 11, E-08222 Terrassa, Barcelona, Spain*

<sup>3</sup>*Institució Catalana de Recerca i Estudis Avançats (ICREA), Passeig Lluís Companys 23, E-08010, Barcelona, Spain*

Non-Hermitian systems exploiting the synergy between the properties of closed-conservative systems and open-dissipative (gain/loss) systems have recently become the playground to uncover unusual physical phenomena. Indeed, the spatial symmetry breaking in such systems allows tailoring the wave propagation at will. Inspired by such property, we propose a feasible approach based on local Hilbert transform to control the field flows in two- or higher dimensional non-Hermitian systems. Moreover, we invent an iterative procedure to reduce the dimensionality of complex refractive index parameter space to two, one or zero dimensions, restricting the complex refractive index within practical limits. The proposal provides a flexible way to systematically design local PT-symmetric systems realizable with a limited collection of realistic materials.

## I. INTRODUCTION

Physical causality is closely related with the celebrated Hilbert Transform (HT). In optics, the HT is well known as the Kramers-Kronig (KK) relations, connecting the real and imaginary parts of the spectrum of the response function of a system [1] in a way that it ensures that response must occur at a later (not earlier) time of its excitation. Such a HT breaks the time symmetry, and accounts for the “invisibility” of the future.

Recently, an analogous HT was proposed in space to define the spatial profile of the complex susceptibility of a system to non-Hermitically engineer a nonisotropic response, thus breaking the spatial symmetry. In one-dimension (1D), space and time are both scalars and therefore the HT in space and time are mathematically equivalent [2]. The invisibility of the future or the absence of the flow of information to the past may be regarded as analogous to the absence of scattering, say backscattering irradiating in the direction opposite to the illumination [3-5]. In two- and three-dimensions, however, the situation becomes more engaged as backscattering (unidirectional invisibility) can be eliminated from different directions. For instance, in a two-dimensional (2D) space, it is possible to manipulate the scattering of an object towards particular directions [6,7] by correspondingly modifying its spatial susceptibility function via the HT.

The spatial symmetry breaking of the system response, on the global scale is extensively studied in the context of Parity-Time (PT)-symmetry to explore novel physical effects [8-18]. Moreover, such symmetry breaking of the spatial response may occur locally, i.e. being different at different spatial positions, which allows engineering of complex directionality fields, with particular topologies such as axisymmetry [19] or following arbitrary vector

Subject Areas: Optics, Photonics

fields being the background potential from periodic, quasiperiodic, to random [20].

Despite some attempts [7,21], yet a practical realization of the HT in space, either in global or local sense, remains a grand challenge. Actual realizations of the spatial HT are severely restricted by the limited available materials that can satisfying the required complex refractive index requirements ( $n_{\text{Re}}, n_{\text{Im}}$ ). With the development of metamaterials, which response function relies on their subwavelength artificial structures rather than to chemical compositions, the possible regime of refractive index profile has been greatly expanded. Thus, metamaterials bring about the opportunity to realize a precise relation between the real and imaginary parts of the response function required by the spatial HT. For instance, metamaterials based on a particular collection of “metachips”, satisfying a given response spectra, allow a spatial HT profile in the microwave regime [22]. However, it is not possible to realize arbitrary relations between real/imaginary parts of susceptibility from a limited collection of real materials. In semiconductor microstructures, the situation is also similar, as actual active materials have a specific relation between index and gain-loss ( $n_{\text{Re}}, n_{\text{Im}}$ ).

The fundamental question that arises is if an actual field of unidirectionality can be implemented, either with a global or local topology, using the HT approach within restricted (realistic) range of complex susceptibility of a material. Arbitrary unidirectional vector fields can be designed by locally modifying the complex susceptibility (or complex refractive index) using the local Hilbert transform. As an example, Fig.1 illustrates such directionality field consisting of a sink and a source. However, the resultant complex index profile demands a large number of actual materials for the practical

realization due to the continuous variation of complex index values in space [see Fig. 1(b) and 1(c)]. To resolve this issue, we propose to introduce restrictions for the complex index values, constraining them around certain particular values or confining them in some particular areas of the parameter space  $(n_{\text{Re}}, n_{\text{Im}})$ . Such a restriction may possibly not limit the field unidirectionality or total invisibility, resulting into a basic scattering reduction. We propose an iterative procedure, to include such constraints to design the locally PT-symmetric systems with realistic index and gain/loss values.

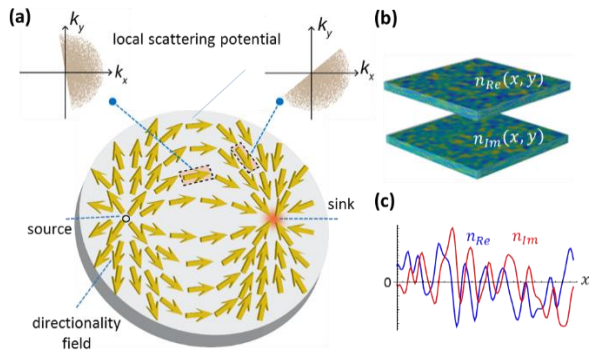


FIG. 1. (color online) Locally modified nonhermitian media providing the local Hilbert transform: (a) Scattering potential of the media,  $n_{\text{Re}}(x, y)$ , modified by local HT to mold the flow of light in the desired direction. Here, the optical media is specifically tailored to create source and sink fields, which involves gain-loss regions,  $n_{\text{Im}}(x, y)$ . The constructed two-dimensional complex potential  $n(x, y) = n_{\text{Re}} + i n_{\text{Im}}$  holds PT-symmetry locally, i.e., at each spatial location in the space to provide a precise control over directional flow (b) 2D complex refractive index profiles of the modified HT media requiring a large number of materials corresponding to different spatial point (c) cross-sectional profile of the complex index.

## II. DIMENSIONALITY RESTRICTIONS

Typical restrictions of the non-Hermitian media to engineer the local HT considered in our study are the following:

(1) HT media as a mixture of two different materials with two different complex refractive indices. Restricting the total filling factor of two materials leads to a 1D manifold in the refractive index in complex refractive index parameter space, while limiting the total filling factor of two materials to some upper bound results in a general 2D manifold of available complex refractive indices, a surface [Fig. 2(a)]. Mixing of chemical components or/and manipulating porosity is a common practice to vary the refractive indices in desired range typically between 1.2 to 2.1 in vapor deposition techniques [23,24].

(2) HT media as a metamaterial build from a continuous family of size-scaled metachips in microwave range [22], which restricts the complex refractive index space to a ring [Fig. 2(b)].

(3) HT media as a “poor man” collection of the discretely size-scaled resonators (for instance, of Helmholtz resonators in acoustics, or microwave metachips), corresponding to a discrete set of points in the complex index space [Fig. 2(c)].

In this way, to show the universality of the method to engineer the desired HT profiles in the restricted parameter space, we analyze these distinct cases, which entail reducing the dimensionality in parameter space of complex refractive indices. For instance, Fig. 2 illustrates the kind of the dimensionality reductions of the three proposed restrictions (a) 2D  $\rightarrow$  2D, (b) 2D  $\rightarrow$  1D and (c) 2D  $\rightarrow$  0D.

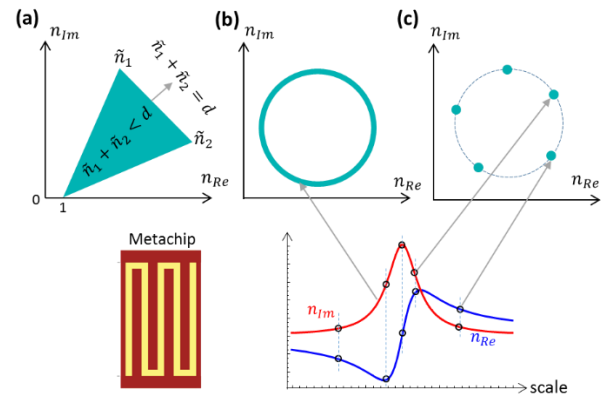


FIG. 2. (color online). Restrictions of the local HT for different restriction dimensionalities: (a) mixture of two different materials with  $\tilde{n}_1, \tilde{n}_2$ ; for instance fixing the total density  $\tilde{n}_1 + \tilde{n}_2 = d$  (solid or liquid -like) gives a line, and mixture of two materials restricting the maximal density  $\tilde{n}_1 + \tilde{n}_2 < d$ , gives an area in complex space, (b) continuum of scalable metachips gives an available ring in  $n$ -complex space, and (c) limited collection of scaled-in-size meta-atoms gives a set of points in complex space (five points in this case).

## III. RESULTS

### A. Restricted Hilbert Transform

To implement the proposed schemes, we apply an iterative procedure. First, we perform a local HT on an arbitrary background potential to create desired directionality flows such as a sink, which requires a large area of real/imaginary values of  $n(\vec{r})$ . Second, we shift the unallowed values of complex of  $n(\vec{r})$  to the restriction area. As this process partially breaks the HT, then we perform the HT again and repeat the procedure. We repeat this iterative procedure until the index values converge. We define a correlation coefficient for the generated vectorial potentials with different restriction dimensionalities to characterize the accuracy and convergence of the restricted HT, which confirm that this iterative approach leads to the converging results in all cases studied. To verify the directionality effect in restricted HT, we perform numerical simulations using the Schrödinger equation (for paraxial optics) for linear

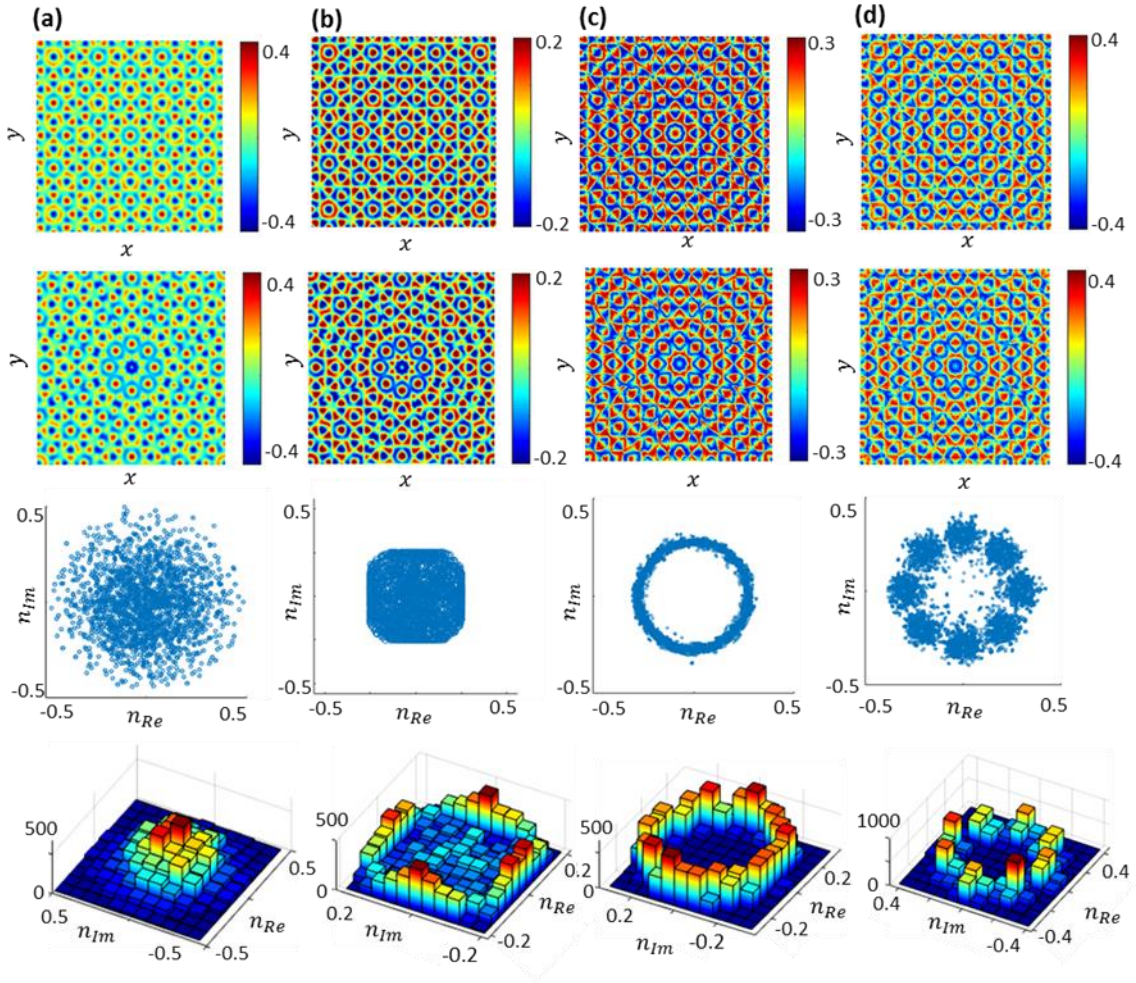


FIG. 3. (color online) Complex refractive index distributions for sink directionality (a) local HT (b,c,d) Restricted local HT (b,c,d) with hexagonal background pattern. In restricted HT cases, the complex index profiles are obtained after fifteen iterations. The first row presents the real part of refractive index, second row depicts the imaginary part obtained from the local HT, and third and fourth rows depict the corresponding restricted index values and density distribution in complex space, respectively.

systems with given complex vectorial potentials. We also perform the full wave simulations to demonstrate the functionality of the proposal beyond the paraxial approximation (see Supplemental Material).

As an example of a possible realization of a restricted HT media, we consider an initial real-valued hexagonal profile,  $n_{Re}(\vec{r})$  [see top-left panel in Fig. 3] and generate the corresponding gain-loss profile,  $n_{Im}(\vec{r})$ , by applying the local HT transform [20] to ensure the converging directionality field in form of sink:  $p(\vec{r}) = -\vec{r}/|\vec{r}|$ . The parameter space of complex refractive index ( $n_{Re}, n_{Im}$ ) provides different material parameters as functions of the spatial location [see Fig. 3(a)]. To realize such complex profiles with available materials, we apply local HT iteratively to restrain the complex index values within physical limits. The results for different restriction dimensionalities are shown in Fig. 3(b-d). The index values in complex space ( $n_{Re}, n_{Im}$ ) illustrate that the iterative procedure precisely limits the refractive indices

within the designated area, ring or a set of points on a ring [see the third row of Fig. 3]. The corresponding density distributions of complex index, plotted in the last row of Fig. 3, also show the spreading of restricted values inside the desired bounds. Note that the restricted HT provides many possible ways to restrict the complex indices during the iterative procedure and some of them are discussed in Supplemental Material. In addition, the procedure is independent of the background potential profile and can be applied to arbitrary initial distribution i.e. quasiperiodic, random, localized etc [see Supplemental Material for random background medium]. Note that iterative procedure can be applied to exclude the gain to achieve analogous directionality fields with only losses in restricted parameter space, thus increasing the feasibility for practical realization.

## B. Coverage of Restricted Hilbert transform

To analyze the robustness and convergence of the iterative procedure, we determine the correlation coefficients in

terms of flow of complex potential generated by HT under different restrictions. We define the correlation coefficient as:  $C = \int p(\vec{r}) \cdot f_k(\vec{r}) d\vec{r} / \sqrt{\int |p(\vec{r})|^2 d\vec{r} \cdot \int |f_k(\vec{r})|^2 d\vec{r}}$  where  $p(\vec{r})$  is the reference flow and  $f_k(\vec{r}) = i(U_k \nabla U_k^* - U_k^* \nabla U_k)$  is the potential flow after  $k$  iterations with the restrictions. For the cases shown in Fig. 3, we assume sink directionality to generate the complex vectorial potentials. Therefore, the reference flow is kept with the form of the sink:  $p(\vec{r}) = -\vec{r}/|\vec{r}|$  to determine the correlation coefficient.

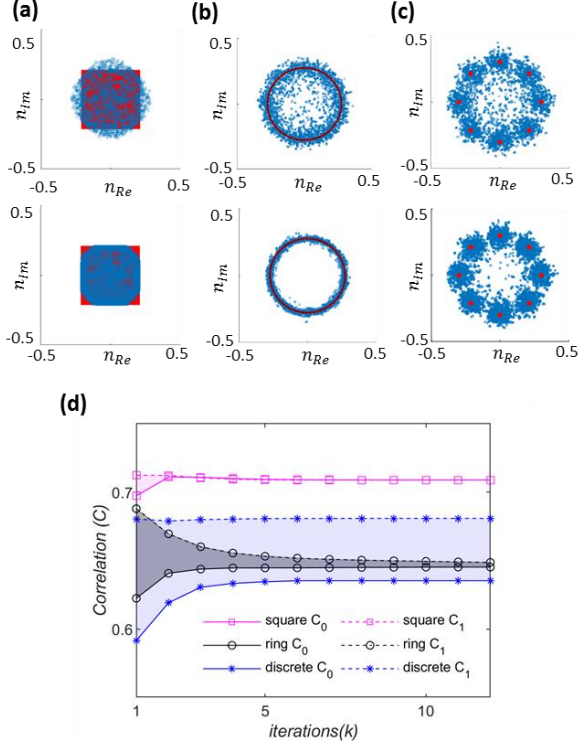


FIG. 4. (color online) Convergence of restricted local Hilbert transform (a-c) first and second rows depict refractive indices in complex space after 1<sup>st</sup> and 12<sup>th</sup> iterations, respectively. The red and blue color illustrate the desired and computed restricted complex refractive index values obtained from local HT, respectively. (d) Correlation coefficients ( $C_0$  solid line ;  $C_1$  dotted line) in terms of flow of the complex potential generated by HT during iterative procedure for different restriction dimensionalities ( $\square$ ) 2D→2D, ( $\circ$ ) 2D→1D, ( $*$ ) 2D→0D.

We expect that the constraints have a weak influence on the pattern of potential flows with reference to sink. Here, we compute two correlation coefficients namely  $C_0$  and  $C_1$  for which  $f_k(\vec{r})$  is calculated from complex refractive distribution obtained by applying HT before and after the restriction at  $k$  iteration, respectively. The difference between  $C_0$  and  $C_1$  estimates the accuracy of the proposed restricted HT. To illustrate the difference of applying the HT before and after restrictions, we present the refractive indices in complex space after 1st and 12th iterations in Figs. 4(a-c). The second row in Figs. 4(a-c) shows the convergence of values of refractive index values in complex space for all cases. In (a), the restricted HT accurately limit the complex refractive indices in desired

ranges. However, for (b,c), the refractive indices somehow spread around the ring and the chosen discrete points. This spreading behavior due to restrictions in complex space may be associated with uncertainty principle i.e. the smaller the restricted area, the larger the spreading. The correlation coefficients  $C_0$  and  $C_1$ , calculated during the iterative procedure, are plotted in Fig. 4(d). In the square case, we obtain exactly the same values for both correlation coefficients after fifteen iterations ensuring 100% accuracy. However, we found  $\sim 1\%$  and  $\sim 5\%$  difference in correlation coefficients for ring and discrete cases, respectively. Note that the difference between correlation coefficients, for the considered restrictions, remains the same regardless of background pattern but the exact correlation values,  $C_0$  and  $C_1$ , depend on the background pattern. For instance, in pure sinusoidal pattern, these values are close to one but lower than unity in the considered hexagonal pattern. We note that the convergence of correlation coefficients requires more iterations when the restriction area shrinks. In the square case, the large restriction area leads to a fast converge, as compared to ring and discrete case. However, the iterative procedure converges after ten iterations in all cases as depicted in Fig. 4(d).

### C. Field evolution in Restricted HT media

To validate the “*Restricted Hilbert transform*” proposal, we performed numerical simulations using paraxial equation of diffraction (equivalent to the Schrodinger equation for a quantum wave function) expressed in the form:

$$\partial_t A(\vec{r}, t) = +i\nabla^2 A(\vec{r}, t) + iU(\vec{r})A(\vec{r}, t) \quad (1)$$

where  $A(\vec{r}, t)$  is slowly varying complex field envelop distributed in space,  $\vec{r}(x, y)$  and evolving in time,  $t$ .  $U(\vec{r}) = n_{Re}(\vec{r}) + in_{Im}(\vec{r})$  is the non-Hermitian potential being  $n_{Re}(\vec{r})$  the real refractive index profile and  $n_{Im}(\vec{r})$  the corresponding imaginary part of the potential obtained from local HT with sink directionality.

We numerically solve Eq. (1) using the split step method for HT media with different restrictions. For the complex refractive index profiles shown in Figs. 3(a-d), the simulated steady-state field distributions are provided in Fig. 5, where a gaussian source is initially placed at an arbitrary position within the modified structure as show in Fig. 5a(i). The system shows initially the transients as depicted in Fig. 5a(ii) but eventually the field is efficiently concentrated around the center in a(iii), due to the sink directionality. The final localized states for different restrictions are shown in (b-d) [see Supplemental Movie for evolution of the field in HT media with different restrictions].

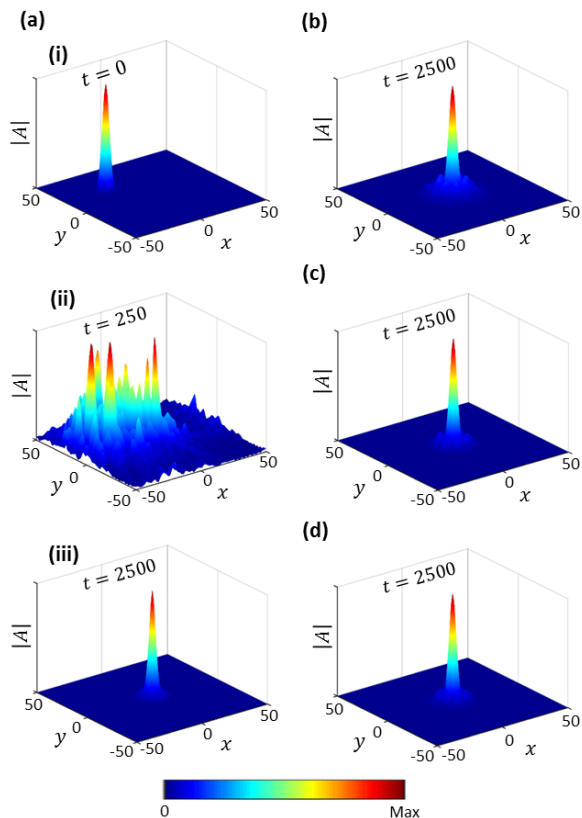


FIG. 5. (color online) Field evolution in modified HT media for sink directionality. The system is excited with a gaussian beam placed at an arbitrary position within the structure as shown in a(i). Numerically calculated transient and final localized states are shown in a(ii) and a(iii), respectively. The steady state distributions for restricted cases are: (b) square area (c) ring (d) a set of discrete points on the ring. The results indicate that gaussian source, initially located at arbitrary position, localizes around the center in all cases after sufficient propagation time.

#### IV. CONCLUSIONS

To conclude, we propose a restricted Hilbert transform for the generation of feasible systems holding local PT-symmetry to manage arbitrary field flows in higher dimensional non-Hermitian systems under a realistic parameter space. In particular, we study restrictions of different dimensionalities from 2D to 1D and 0D to achieve the refractive indices for locally PT-symmetric systems within desired ranges. The procedure provides a substantial control over the chosen index values as compared to conventional spatial Kramers-Kronig relation, and the constructed index profiles can be experimentally realized with limited collection of realistic materials by locally tuning the real and imaginary part of dielectric media. It is worth mentioning that discrete HT transform requires minimum three different materials, three unaligned points in susceptibility complex plane for realization. It also offers a general design strategy to implement any desired field configuration in a broad class of non-Hermitian systems conceptually different from existing coordinate transformation approaches[25-28]. We believe that the proposal opens new possibilities to

practically realize the wave dynamics of linear and nonlinear physical systems based on engineered HT media with realistic index and gain/loss values.

The work described in here is partially supported by King Abdullah University of Science and Technology (KAUST) Office of Sponsored Research (OSR) under Award No. OSR-2016-CRG5-2950 and KAUST Baseline Research Fund BAS/1/1626-01-01. K. Staliunas acknowledges the support of Spanish Ministerio de Economía y Competitividad (FIS2015-65998-C2-1-P) and European Union Horizon 2020 Framework EUROSTARS (E10524 HIP-Laser).

\*ying.wu@kaust.edu.sa

†kestutis.staliunas@icrea.cat

#### References:

- [1] J. D. Jackson, *Classical Electrodynamics* (Wiley, 3rd Edition, 1999).
- [2] S. A. R. Horsley, M. Artoni, and G. C. La Rocca, *Spatial Kramers-Kronig relations and the reflection of waves*, Nat. Photon. **9**, 436 (2015).
- [3] S. Longhi, *Half-spectral unidirectional invisibility in non-Hermitian periodic optical structures*, Opt. Lett. **40**, 5694 (2015).
- [4] S. Longhi, *Wave reflection in dielectric media obeying spatial Kramers-Kronig relations*, Europhys. Lett. **112**, 64001 (2015).
- [5] S. A. R. Horsley, C. G. King, and T. G. Philbin, *Wave propagation in complex coordinates*, J. Opt. **18**, 044016 (2016).
- [6] Z. Hayran, R. Herrero, M. Botey, H. Kurt, and K. Staliunas, *Invisibility on demand based on a generalized Hilbert transform*, Phys. Rev. A **98**, 013822 (2018).
- [7] Z. Hayran, R. Herrero, M. Botey, H. Kurt, and K. Staliunas, *All-Dielectric Self-Cloaked Structures*, ACS Photon. **5**, 2068 (2018).
- [8] K. G. Makris, R. El-Ganainy, D. N. Christodoulides, and Z. H. Musslimani, *Beam dynamics in PT symmetric optical lattices*, Phys. Rev. Lett. **100**, 103904 (2008).
- [9] A. Guo, G. J. Salamo, D. Duchesne, R. Morandotti, M. Volatier-Ravat, V. Aimez, G. A. Siviloglou, and D. N. Christodoulides, *Observation of PT-symmetry breaking in complex optical potentials*, Phys. Rev. Lett. **103**, 093902 (2009).
- [10] C. E. Ruter, K. G. Makris, R. El-Ganainy, D. N. Christodoulides, M. Segev, and D. Kip, *Observation of parity-time symmetry in optics*, Nat. Phys. **6**, 192 (2010)
- [11] S. Longhi, *Bloch oscillations in complex crystals with PT symmetry*, Phys. Rev. Lett. **103**, 123601 (2009).
- [12] Z. Lin, H. Ramezani, T. Eichelkraut, T. Kottos, H. Cao, and D. N. Christodoulides, *Unidirectional invisibility induced by PT-symmetric periodic structures*, Phys. Rev. Lett. **106**, 213901 (2011).
- [13] Y. D. Chong, L. Ge, and A. D. Stone, *PT-symmetry breaking and laser absorber modes in optical scattering*

systems, Phys. Rev. Lett. **106**, 093902 (2012).

[14] L. Feng, Y.-L. Xu, W. S. Fegadolli, M.-H. Lu, J. E. Oliveira, V. R. Almeida, Y.-F. Chen, and A. Scherer, *Experimental demonstration of a unidirectional reflectionless parity–time metamaterial at optical frequencies*, Nat. Mater. **12**, 108 (2012).

[15] B. Peng, S. K. Ozdemir, F. Lei, F. Monifi, M. Gianfreda, G. L. Long, S. Fan, F. Nori, C. M. Bender, and L. Yang, *Parity–time-symmetric whispering-gallery microcavities*, Nat. Phys. **10**, 394 (2014).

[16] L. Feng, R. El-Ganainy, and L. Ge, *Non-Hermitian photonics based on parity–time symmetry*, Nat. Photon. **11**, 752 (2017).

[17] K. G. Makris, A. Brandstötter, P. Ambichl, Z. H. Musslimani, and S. Rotter, *Wave propagation through disordered media without backscattering and intensity variations*, Light Sci. Appl. **6**, e17035 (2017).

[18] R. El-Ganainy, K. G. Makris, M. Khajavikhan, Z. H. Musslimani, S. Rotter, and D. N. Christodoulides, *Non-Hermitian physics and PT symmetry*, Nat. Phys. **14**, 11 (2018).

[19] W. W. Ahmed, R. Herrero, M. Botey, and K. Staliunas, *Locally parity-time-symmetric and globally parity-symmetric systems*, Phys. Rev. A **94**, 053819 (2016).

[20] W. W. Ahmed, R. Herrero, M. Botey, Z. Hayran, H. Kurt, and K. Staliunas, *Directionality fields generated by a local Hilbert transform*, Phys. Rev. A **97**, 033824 (2018).

[21] W. Jiang, Y. Ma, Y. Jun, G. Yin, W. Wu, and W. He, *Deformable broadband metamaterial absorbers engineered with an analytical spatial Kramers-Kronig permittivity profile*, Laser Photon. Rev. **11**, 1600253 (2017).

[22] D. Ye, C. Cao, T. Zhou, J. Huangpu, G. Zheng, and L. Ran, *Observation of reflectionless absorption due to spatial Kramers–Kronig profile*, Nat. Commun. **8**, 51 (2017).

[23] A. Thelen, *Design of optical interference coatings* (McGraw-Hill, New York, 1989).

[24] T. Tolenis, L. Grinevičiūtė, R. Buzelis, L. Smalakys, E. Pupka, S. Melnikas, A. Selskis, R. Drazdys, and A. Melninkaitis, *Sculptured anti-reflection coatings for high power lasers*, Opt. Mater. Express **7**, 1249 (2017).

[25] J. B. Pendry, D. Schurig, and D. R. Smith, *Controlling Electromagnetic Fields*, Science, **312**, 1780 (2006).

[26] U. Leonhardt, *Optical Conformal Mapping*, Science **312**, 1777 (2006).

[27] H. Y. Chen, C. T. Chen, and P. Sheng, *Transformation optics and metamaterials*, Nat. Mater. **9**, 387 (2010).

[28] L. Xu and H. Chen, *Conformal transformation optics*, Nat. Photon. **9**, 15 (2015).